αA-Crystallin Interacting Regions in the Small Heat Shock Protein, αB-Crystallin †

ARTICLE *in* BIOCHEMISTRY · JANUARY 2005

Impact Factor: 3.02 · DOI: 10.1021/bi048151s · Source: PubMed

4 AUTHORS, INCLUDING:

Santhoshkumar Puttur
University of Missouri
42 PUBLICATIONS **728** CITATIONS
SEE PROFILE

Krishna Sharma
University of Missouri
48 PUBLICATIONS **778** CITATIONS
SEE PROFILE

αA-Crystallin Interacting Regions in the Small Heat Shock Protein, αB-Crystallin†

Yellamaraju Sreelakshmi, Puttur Santhoshkumar, Jaya Bhattacharyya, and K. Krishna Sharma*

Departments of Ophthalmology and Biochemistry, University of Missouri, Columbia, Missouri 65212

Received August 26, 2004; Revised Manuscript Received October 12, 2004

ABSTRACT: Amino acid sequences of αB-crystallin, involved in interaction with αA-crystallin, were determined by using peptide scans. Positionally addressable 20-mer overlapping peptides, representing the entire sequence of αB-crystallin, were synthesized on a PVDF membrane. The membrane was blocked with albumin and incubated with purified αA-crystallin. Probing the membrane with αA-crystallin-specific antibodies revealed residues 42−57, 60−71, and 88−123 in αB-crystallin to interact with αA-crystallin. Residues 42−57 and 60−71 interacted more strongly with αA-crystallin than the 88−123 sequence of αB-crystallin. Binding of one of the αB peptides (42−57) to αA-crystallin was also confirmed by gel filtration studies and HPLC analysis. The αB-crystallin sequences involved in interaction with αA-crystallin were distinct from the chaperone sites reported earlier as binding of the αB sequence from residues 42−57 does not alter the chaperone-like function of αA-crystallin. To identify the critical residues involved in interaction with αA-crystallin, R50G and P51A mutants of αB-crystallin were made and tested for their ability to interact with αA-crystallin. The oligomeric size and hydrophobicity of the mutants were similar. Circular dichroism studies showed that the P51A mutation increased the α-helical content of the protein. While the αBR50G mutant showed chaperone-like activity similar to wild-type αB, αBP51A showed reduced chaperone function. Fluorescence resonance energy transfer studies showed that the P51A mutation decreased the rate of subunit exchange with αA by 63%, whereas the R50G mutation reduced the exchange rate by 23%. Similar to wild-type αB, αB-crystallin peptide (42−57) effectively competed with αBP51A and αBR50G for interaction with αA. Thus, our studies showed that the αB-crystallin sequence (42−57) is one of the interacting regions in αB and αA oligomer formation.

α-Crystallin, a predominant eye lens protein, is a member of the small heat shock protein (sHSP)[1] family (*1*). Like other members of this family, α-crystallin exhibits chaperone-like activity by suppressing aggregation of denaturing proteins (*2*, *3*) and, in some instances, protects the biological activity of enzyme proteins as well (*4*). Data suggest that α-crystallin exists as a polydisperse aggregate with an average molecular mass of 800 kDa and is composed of two types of subunits, designated αA- and αB-crystallins (*5*). Each subunit has a molecular mass of 20 kDa, and αA and αB subunits are arranged in the aggregate in yet to be fully understood organization. The α-crystallin molecule is a dynamic aggregate with the subunits dissociating and reassociating constantly (*5*−*9*). Van den Oetelaar et al. (*9*) have shown that the subunits in an α-crystallin molecule exchange with a new set of subunits in approximately 24 h. However, studies by Sun et al. (*6*) revealed that the exchange is a fast process and is temperature-dependent, with the exchange being faster at 37 °C than at 25 °C. α-Crystallin subunits can form homooligomeric and heterooligomeric complexes with a high degree of plasticity in their quaternary structure (*10*). The heterooligomer has a greater thermal stability than either homooligomer alone (*10*, *11*). It has been suggested that, in vivo, α-crystallin mainly exists as a heterooligomer of αA- to αB-crystallin in a 3:1 ratio (*10*, *11*). There is ample evidence to show that the interaction between αA- and αB-crystallins is essential to form structurally stable complexes (*13*, *14*). However, little is known about the actual contact points or recognition sites between these subunits. Given the fact that the crystal structure of either αA- or αB-crystallin is unknown, investigation of contact sites between the subunits will yield valuable information for understanding the structure−function of α-crystallin. Such data can also be used in the α-crystallin homology modeling studies since the crystal structure of related proteins is known (*15*, *16*).

Removal of the first 63 residues of the N-terminal domain of αA-crystallin resulted in a reduction in its size from an average molecular mass of 800 kDa to 60 kDa (*17*). But, truncation of the first 19 residues does not result in a significant change in the size of αA-crystallin (*8*). Other sHSPs such as HSP 12.2 and HSP 12.3 contain only a α-crystallin domain with a very short N-terminal region and no C-terminal tail; they exist as tetramers (*18*). These studies establish the critical role played by the N-terminal region in oligomerization of low-molecular-mass species into functional high-molecular-mass complexes.

† This work was supported by National Institutes of Health Grants EY 11981 and EY 14795, a grant-in-aid from Research to Prevent Blindness (RPB), and a Lew Wasserman Merit Award (to K.K.S. from RPB). Portions of this work were presented at the annual meeting of the Association for Research in Vision and Ophthalmology in 2001.

* To whom correspondence should be addressed. Fax: 573-884-4100. Phone: 573-882-8478. E-mail: sharmak@health.missouri.edu.

[1] Abbreviations: sHSP, small heat shock proteins; CS, citrate synthase; ADH, alcohol dehydrogenase; bis-ANS, 1,1′-bis(4-anilino)-naphthalene-5,5′-disulfonic acid; PBS, phosphate-buffered saline; FRET, fluorescence resonance energy transfer; SAED, sulfosuccinimidyl 2-(7-azido-4-methylcoumarin-3-acetamido)ethyl-1,3′-dithiopropionate; 1,5-AZNS, 1-azidonaphthalene-5-sulfonate.

10.1021/bi048151s CCC: $27.50
Published on Web 11/25/2004

On the other hand, using yeast two-hybrid (*19*, *20*) and mammalian two-hybrid systems (*21*), the entire C-terminal domain of αB-crystallin has been identified as the domain responsible for interaction with αA-crystallin. The two-hybrid system (yeast or mammalian), however, can give false positives since transient interactions are indistinguishable from physiologically relevant interactions between the proteins (*22*). Furthermore, the two-hybrid system is not amenable for identification of epitopes (<20 amino acid regions) in proteins that are involved in subunit interaction. Therefore, we studied the αA- and αB-crystallin recognition sites using peptide scans.

The peptide scan method for studying the protein−protein interactions uses overlapping peptides that encompass the entire subunit of an oligomeric protein, and these peptides are subsequently tested for binding to the interacting subunits/protein (*23*−*27*). With this approach, since the peptide sequence at each spot on membrane is already known, the location of the peptide sequence (as well as the binding site) can be immediately identified in one of the native proteins. The peptide scanning method has been successfully used to identify binding sites in a number of proteins that interact with molecular chaperone DnaK (*24*), to map the adult hemoglobin B chain and A chain interaction (*25*), and to map the interleukin-10/interleukin-10 receptor combining sites (*26*). In those studies, peptide libraries of 7− 20 residues were screened. The results of those studies also corroborated the structural data obtained from X-ray crystallographic studies.

In the present study, we used the peptide scan method to determine the αA-crystallin interaction sites in αB-crystallin. We show that two regions in αB-crystallin, spanning from residues 42−57 and 60−71 (named as recognition sequence 1 and 2, respectively), are particularly involved in interaction with αA-crystallin. To further identify the critical residues involved in αA−αB interaction, we mutated recognition sequence 1 (RS-1) in αB-crystallin that interacted with αA-crystallin at R50 with G and P51 with A. We studied the effect of mutation on structure−function properties of αB-crystallin. The Arg residue was chosen for mutation study because of its charge. Replacement of this residue with a small and neutral amino acid such as Gly will provide information about the role of charge interactions in oligomer formation. Because Pro is a known β-sheet breaker (*28*), replacing Pro with Ala (an α-helix former) allows investigation of the role played by the structural elements on the interacting properties of αB-crystallin. Of the two mutations, we found that the P51A mutation led to slow subunit exchange with αA (63% slower compared to wild type).

EXPERIMENTAL PROCEDURES

Materials. Bovine lens αA-crystallin was prepared according to the method previously described (*29*). αA-Crystallin antibody was a gift from Dr. Richard Cenedella (College of Osteopathic Medicine, Kirksville, MO). Super-Signal West Dura Extended Duration substrate was purchased from Pierce Chemical Co. (Rockford, IL). Peptides and the peptide scan membrane were supplied by Invitrogen Corp. Twenty amino acid long peptides were synthesized within defined spots on the membrane in a configuration which mimics the standard 96-well microtiter plate array format (standard Fmoc chemistry was used to obtain αB-crystallin peptide scan). The peptides were C-terminally attached to a PVDF membrane; each spot contained about 10 nmol of each peptide. The peptide library encompassed the entire αB-crystallin sequence, and each peptide overlapped its consecutive neighbor by 18 residues.

Screening of αB-Crystallin Peptide Scans for Binding of αA-Crystallin. The peptide membrane was rinsed with methanol for 10 min, followed by sodium phosphate buffer, pH 7.4, plus 0.9% NaCl (PBS) for 20 min. The membrane was treated with 1% bovine serum albumin for 1 h to saturate all nonspecific binding sites. Purified bovine αA-crystallin (5 mg/10 mL of PBS) was allowed to interact with the peptide membrane at 37 °C for 4 h with gentle shaking. The unbound αA-crystallin was removed with three PBS washes. The peptide-bound αA-crystallin was electrotransferred (*30*) onto a nitrocellulose membrane. The transferred αA-crystallin was detected with αA-crystallin-specific antibody using a chemiluminescence blotting substrate kit according to the instructions from the supplier (Pierce).

Confirmation of the αB-Crystallin Peptide Interaction with αA-Crystallin. The interaction of the peptide (TSLSPFYLRPPSFLRA, residues 42−57 of αB-crystallin, named as recognition sequence 1 or RS-1) with αA-crystallin was confirmed in following manner. Synthetic peptide (100 μg) was mixed with purified bovine lens αA-crystallin (500 μg) and incubated in 50 mM phosphate, pH 7.5, plus 0.1 M NaCl (buffer A) at 37 °C. After 4 h, the mixture was subjected to gel filtration on a BIOSEP SEC 3000 column (Phenomenex) which had been previously equilibrated with buffer A. The elution was monitored at 280 nm, and 0.5 mL fractions were collected. The αA-crystallin peak was collected and concentrated, and the sample was analyzed by a reverse-phase HPLC on a C18 column (Vydac 218TP104 Separations Group, Hesparia, CA) using a 0−80% linear gradient formed between water and acetonitrile containing 0.1% TFA. A flow rate of 1 mL/min was maintained, and the elution was monitored at 220 nm. Peptide (100 μg) by itself and αA-crystallin (100 μg) were injected onto the column as controls. As additional controls, the binding of a reverse sequence of RS-1 (ARLFSPPRLYFPSLST, 100 μg) and another hydrophobic sequence of αB-crystallin (MDIAIHHPWIRRPFFPFH, residues 1−18, 100 μg) with αA-crystallin (500 μg) was investigated.

In another experiment, 100 μg of αA-crystallin and 100 μg of the peptide TSLSPFYLRPPSFLRAPSWF (Trp-containing RS-1 sequence, named as peptide 22) were mixed in buffer A. Intrinsic fluorescence spectra of the sample at 0 time and after 16 h at 37 °C were recorded in a Jasco FP 750 spectrofluorometer (excitation 295 nm, emission 300−400 nm; bandwidth of 5 nm). A mixture of peptide 22 and αA-crystallin incubated for 16 h at 37 °C was then passed through a gel filtration column (BIOSEP SEC 3000 column equilibrated in buffer A), and the αA-crystallin peak was collected and subjected to intrinsic fluorescence analysis as above. The fluorescence was also recorded for the peptide and αA-crystallin by themselves at 0 time and after 16 h incubation.

Construction, Expression, and Purification of Wild-Type αA-, Wild-Type αB- and Mutant αB-Crystallins. Human αA- and αB-crystallin cDNA (obtained from Dr. J. M. Petrash, Washington University, St. Louis, MO) were cloned into a

pET23d vector (Novagen) at the *Nco*I/*Hin*dIII site. αBR50G and αBP51A mutants were constructed using a Quik-Change site-directed mutagenesis kit (Stratagene). Mutations were confirmed by automated DNA sequencing. The proteins were expressed in *Escherichia coli* BL21(DE3)pLysS cells (Invitrogen), as described by Horwitz et al. (*31*), and were purified according to the method previously described (*32*). The purity of the recombinant proteins was checked by SDS−PAGE, and the mass was confirmed by ESI mass spectrometry.

Molecular Size Determination. The oligomer size was determined by gel filtration of 100 μg each of wild-type and αB mutants on a BIOSEP SEC 4000 (Phenomenex) column equilibrated with 0.05 M phosphate buffer containing 0.15 M NaCl, pH 7.4. The mass was calculated from the calibration curve generated by using molecular weight markers (ranging from M_r 700000 to 29000) from Sigma.

Tryptophan Fluorescence Measurements. The intrinsic fluorescence spectra of the wild-type and mutant αB-crystallins were recorded using a Jasco FP-750 spectrofluorometer. Protein samples of 0.2 mg/mL in 0.05 M phosphate buffer containing 0.15 M NaCl, pH 7.4, were excited at 295 nm, and emission spectra were recorded between 300 and 400 nm.

Bis-ANS Fluorescence Measurements. To 0.2 mg/mL wild-type and mutant proteins taken in 0.05 M phosphate buffer containing 0.15 M NaCl was added 10 μM bis-ANS. The samples were excited at 385 nm, and the emission spectra were recorded from 400 to 600 nm using a Jasco spectrofluorometer.

Circular Dichroism Studies. Changes in protein secondary structure were measured by far- and near-UV CD spectra in an AVIV circular dichroism spectrometer. Proteins were used at a concentration of 0.2 mg/mL for far-UV and at 3 mg/mL for near-UV measurements. The reported CD spectra are the average of five scans.

Chaperone-like Activity. The ability of the wild-type, mutant proteins, and the αA−RS-1 peptide complex to prevent protein aggregation was determined using citrate synthase (CS) and alcohol dehydrogenase (ADH) as the substrates.

CS Aggregation Assay. CS, 75 μg (Roche Molecular Biochemicals), in 1 mL of 40 mM Hepes−KOH buffer (pH 7.4) was heated at 43 °C for 1 h in the presence of 35 and 50 μg of wild-type and mutant proteins. The extent of aggregation was measured by monitoring the light scattering at 360 nm in a Shimadzu spectrophotometer. In a separate experiment, aggregation of CS (75 μg) was monitored in the presence of 20 and 45 μg of the αA−RS-1 peptide complex. Wild-type αA (45 μg) was used as a control.

ADH Aggregation Assay. Aggregation of ADH, 800 μg (Sigma), was carried out at 37 °C in 0.05 M phosphate buffer containing 0.15 M NaCl and 100 mM EDTA in the presence of 20 μg of either wild-type or mutant αB-crystallins. Light scattering was measured up to 100 min. In a separate assay, ADH (400 μg) aggregation was monitored in the presence of 20 and 45 μg of the αA−RS-1 peptide complex. αA (45 μg) and RS-1 peptide (50 μg) were used as controls. ADH was also incubated in the presence of RS-1 peptide (50 μg) to see if it possesses any chaperone-like activity.

Determination of Protein Stability. The stability of wild-type αB and the αB mutants was determined at 37 and 43 °C, the temperatures at which the chaperone assays were done. αB wild type and mutants (100 μg each) were incubated in 0.05 M phosphate buffer containing 0.15 M NaCl, pH 7.4, separately in the absence of target protein, and absorbance at 360 nm was monitored for 60 min.

Labeling of Recombinant αA-, αB-, and αB-Crystallin Mutants. Purified αA-crystallin was labeled with Alexa fluor 488, and wild-type and mutant αB-crystallins were labeled with Alexa fluor 350 according to the manufacturer's (Molecular Probes) recommendations. Briefly, α-crystallin subunits were mixed with Alexa fluor dye in PBS supplemented with 100 mM sodium bicarbonate. The reaction was allowed to proceed for 1 h at room temperature. Labeled proteins were separated from excess Alexa fluor dye by passing through a gel (Bio-Gel P-30) supplied with the kit. The first fluorescent peak, representing the labeled protein, was collected, and the slower running free dye band was discarded.

Fluorescence Resonance Energy Transfer Measurements. The rate of subunit exchange between αB-crystallin (both wild type and mutants) and αA-crystallin was measured using the fluorescence resonance energy transfer (FRET) technique. Alexa fluor 350-conjugated wild-type αB-crystallin and its mutants were used as the energy donors, and Alexa fluor 488-conjugated αA-crystallin was the energy acceptor. αB-350, αBP51A-350, and αBR50G-350 [25 μg each (separately)] and 75 μg of αA-labeled with Alexa flour 488 were taken in PBS (a 3:1 αA to αB ratio was used to mimic the in vivo situation,) and the sample was incubated at 37 °C. The subunit exchange was monitored by exciting the sample at 346 nm (excitation wavelength for Alexa fluor 350) and measuring the emission spectra from 400 to 600 nm (emission for Alexa fluor 488 is at 520 nm) for 2−3 h. As the exchange progresses, there is a decrease in the fluorescence intensity of the donor with a concomitant increase in acceptor fluorescence. The rate of subunit exchange was calculated as described by Bova et al. (*8*).

To examine the ability of mutant proteins to replace wild-type αB from αA-αB oligomer, 25 μg of αB (wild type, unlabeled) and 75 μg of αA-488 were taken in PBS, and the sample was incubated at 37 °C for 4 h. Then, 25 μg of αB (wild type or mutants labeled with Alexa fluor 350) was added to the reaction mix, and the time-dependent decrease in donor fluorescence and concomitant increase in acceptor fluorescence was monitored for 3−4 h.

To check the effect of RS-1 peptide on subunit exchange between αA and αB, 25 μg of αBP51A-350, 75 μg of αA-488, and 25 μg of αB (unlabeled as a control) or 75 or 100 μg of RS-1 peptide were taken in PBS, and the subunit exchange was monitored at 37 °C. Similarly, the reaction was done with αBR50G-350.

Protein concentrations were determined using the BCA protein assay reagent (bicinchoninic acid, Pierce) using BSA as a standard. We also standardized this method to measure peptide concentration and found it to be satisfactory.

RESULTS

We screened PVDF membrane-bound αB-crystallin peptides for αA-crystallin binding. The αB-crystallin peptide array was composed of 20-mer peptides overlapping by 18 residues and thus representing all potential binding sites for

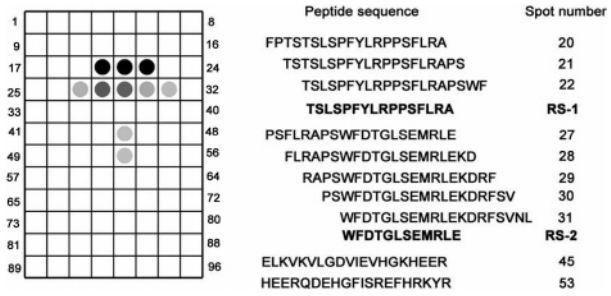

FIGURE 1: Binding of αA-crystallin to αB-crystallin peptide scans. αB-peptide scans were screened for αA binding according to the procedure discussed in Experimental Procedures. The representative peptide spots are marked in the grids. The extent of binding is indicated by the intensity of spots. Darker spots indicate stronger interactions. Peptide sequences corresponding to the spots are also indicated.

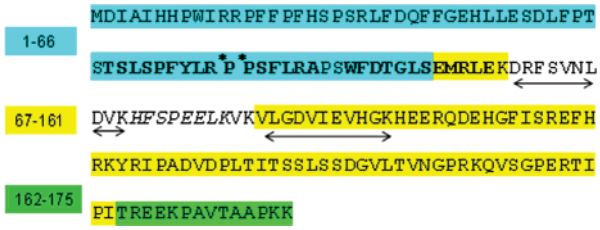

FIGURE 2: Human αB-crystallin sequence showing the αA-crystallin recognition sites (in bold) identified by peptide scan assay. Residues in bold indicate recognition sites 1 and 2 identified in this study. The sequence also shows the N-terminal domain (1−66 residues), α-crystallin, or the C-terminal domain (67−161) and C-terminal extension (162−175). R^* and P^* indicate the residues mutated in this study. The unshaded region indicates the chaperone site identified earlier (*37*). Residues underlined with arrows indicate the bis-ANS binding sites, and residues in italics indicate the 1,5-AZNS binding site and are taken from ref *40*.

αA-crystallin. The peptide scan was incubated with purified αA-crystallin. After an equilibration time of 4 h, the bound protein was electrotransferred and subjected to immunodetection. Figure 1 shows a computer-processed image of the peptide scan, and it also displays the sequence of peptide spots that interacted with αA-crystallin. Since the sequence of the peptides at those positions is known, we inferred that αB-crystallin peptides at spots 20−22 and 27−31 strongly interacted with αA-crystallin. On the basis of the sequences of peptides at spots 20−22 and 27−31, we have designated the TSLSPFYLRPPSFLRA and WFDTGLSEMRLE regions in αB-crystallin as recognition sites (RS) 1 and 2, respectively (Figure 2). Very weak interactions were also observed between αA-crystallin and peptide spots at positions 45 and 53, corresponding to residues 88−107 and 104−123, respectively, in αB-crystallin.

Confirmation of Interaction of αB-Crystallin Peptide with αA-Crystallin. The interaction of αB peptide with αA-crystallin was confirmed by gel filtration and HPLC analysis. Two peaks were observed when a mixture of αA-crystallin and synthetic peptide (RS-1), corresponding to one of the αB recognition sites, was subjected to gel filtration (Figure 3A). In Figure 3A, the peak eluting at 12.45 min is the complex between αA-crystallin and RS-1 peptide, whereas the peak at 23.38 min represents the unbound RS-1 peptide in the mixture (or the peptide by itself, shown for comparison). αA-crystallin alone also elutes at 12.45 min from this column (data not shown). Reverse-phase HPLC analysis of the protein peak eluting at 12.45 min confirmed the binding of RS-1 peptide to αA-crystallin. In Figure 3B, the peak eluting at 34.02 min is the RS-1 peptide, whereas the peak at 43.77 min represents αA-crystallin. A C18 column analysis of an aliquot of a mixture of RS-1 peptide and αA-crystallin prior to gel filtration is shown in Figure 3C and depicts the elution time for RS-1 peptide and αA-crystallin. However, when the reverse sequence of RS-1 peptide was used in place of RS-1 peptide, there was no evidence of this peptide binding to αA-crystallin. C18 column analysis (Figure 3E) showed only αA-crystallin as a component of the high molecular weight protein peak from the BIOSEP SEC 3000 column (Figure 3D). A similar result was obtained when hydrophobic αB-crystallin peptide 1−18 was used (data not shown). Taken together, these data indicate that the binding of RS-1 peptide to αA-crystallin is sequence-specific.

Spectroscopic Analysis of the Interaction between αB-Crystallin Peptide and αA-Crystallin. The interaction between the RS-1 region and αA-crystallin was further confirmed by testing the binding of an extended RS-1 peptide (TSLSPFYLRPPSFLRAPSWF; peptide 22 from the peptide scan, Figure 1) containing a Trp residue. When peptide 22 was mixed with purified αA-crystallin in buffer A and the intrinsic fluorescence spectra of the mixture was recorded at 0 time, an emission maximum at 355 nm was observed (Figure 4A). This was primarily due to the excess concentration of the peptide (36.9 nmol of peptide compared to 5 nmol of αA-crystallin), which also has an emission maximum at 356 nm, masking the 340 nm emission maximum of native αA-crystallin. The fluorescence spectra recorded for αA-crystallin and peptide 22 separately at 16 h are similar to that at the beginning of the experiment (data not shown). Since the reaction mixture also contained an excess of peptide 22 that was not bound to αA-crystallin, we separated the free peptide from the αA-crystallin−peptide complex by gel filtration to investigate whether binding of peptide 22 alters Trp fluorescence. The complex was then subjected to fluorescence analysis. The result is shown in Figure 4B. The Trp emission spectra for the purified complex of αA-crystallin−peptide 22 displayed an emission maximum at 345 nm, suggesting that the Trp of peptide 22 is now partially buried as a consequence of interaction with αA-crystallin.

Chaperone-like Activity of the αA-RS-1 Peptide Complex. It was of interest to know whether binding of RS-1 peptide will alter the chaperone-like function of αA-crystallin. If the chaperone site and RS-1 interaction site in αA-crystallin are the same, then we expect the αA−RS-1 peptide complex to show significantly reduced chaperone-like activity. Figure 5 shows EDTA-induced aggregation of ADH at 37 °C in the presence and absence of the αA−RS-1 complex. The αA−RS-1 complex at 20 μg partially suppressed the aggregation of ADH (400 μg). When a higher concentration (45 μg) of the αA−RS-1 complex was used, the extent of suppression of the aggregation of ADH was similar to that observed with αA-crystallin (45 μg) without bound RS-1. RS-1 peptide by itself did not show any aggregation. Also, RS-1 peptide (50 μg) did not show any chaperone-like activity when incubated along with ADH. A similar result was obtained when the chaperone-like activity of the αA−RS-1 complex was checked against thermal aggregation of citrate synthase (data not shown).

Structural Characterization of αB Mutants. In the present study, both the wild-type and mutant αB-crystallins ex-

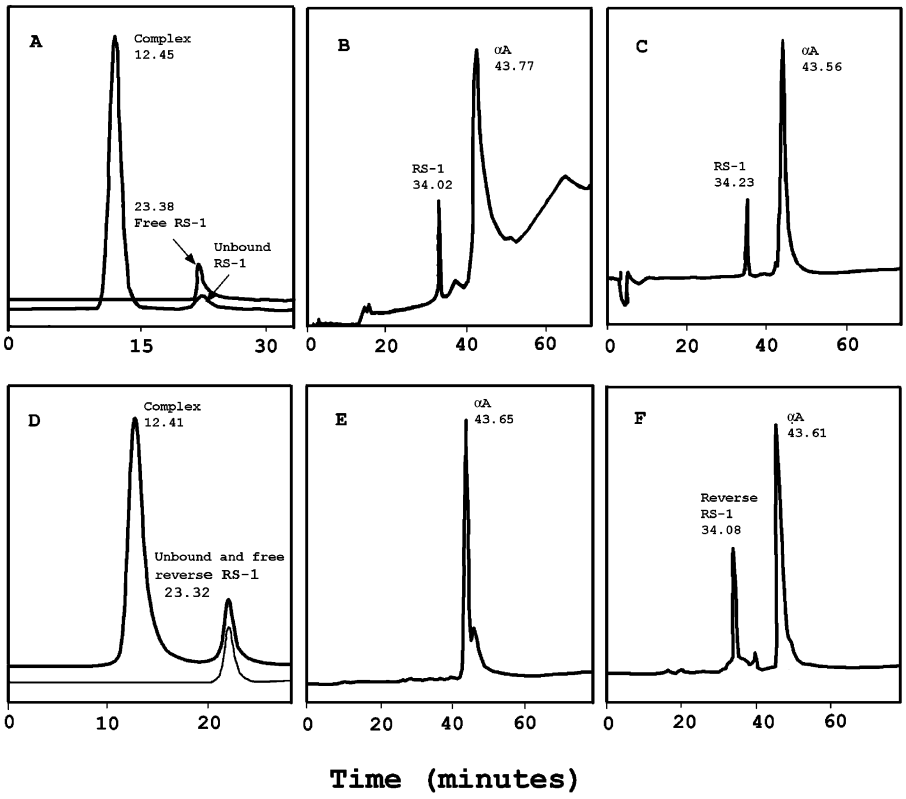

FIGURE 3: Chromatographic analysis of αA-crystallin, RS-1 peptide, and reverse RS-1 peptide. **(**A**)** Elution profile of the αA-crystallin−RS-1 mixture and RS-1 on a BIOSEP SEC 3000 HPLC column. The experimental detail is included in the text. (B**)** HPLC analysis of the 12.45 min (complex) peak from panel A using a C18 column. The peak eluting at 34.02 min is the RS-1 peptide whereas the peak at 43.77 min is that of αA-crystallin. (C**)** HPLC analysis of an aliquot of a mixture of RS-1 peptide and αA-crystallin prior to gel filtration. (D) Elution profile of the αA-crystallin−reverse RS-1 mixture and reverse RS-1 on a BIOSEP SEC 3000 column. (E) C18 HPLC analysis of the 12.41 min (complex) peak from panel D. The peak eluting at 43.65 min is αA-crystallin. Note the absence of the reverse RS-1 peptide peak. (F) C18 HPLC analysis of an aliquot of a mixture of reverse RS-1 peptide and αA-crystallin prior to gel filtration.

pressed in *E. coli* BL21(DE3)pLysS cells were purified by gel filtration and ion-exchange chromatography. The electrospray mass spectrometry revealed molecular masses of 20158.9, 20059.7, and 20132.8 Da, expected molecular masses for wild type and αBR50G and αBP51A mutants, respectively. To determine whether mutation caused any change in the oligomeric size of the crystallins, the purified wild-type as well as αB mutant proteins were chromatographed on a BIOSEP SEC 4000 column. Both wild-type and mutant proteins showed similar elution profiles (Figure 6), corresponding to an oligomeric mass of 6.1×10^5 Da. This finding indicates that the mutation did not affect the homooligomerization of the proteins.

Intrinsic fluorescence spectra (Figure 7) exhibited similar wavelength maxima (343 nm) for wild-type αB and the mutants. However, compared to the fluorescence intensity for wild-type αB, there was a 30% reduction for αBP51A, followed by a 45% reduction for αBR50G. Bis-ANS is a hydrophobic molecule whose fluorescence intensity increases on binding to the hydrophobic regions in proteins. Only a marginal decrease was observed in the binding of bis-ANS to αBP51A and αBR50G as compared to wild-type αB (data not shown). These results indicate that the mutation did not affect the available hydrophobic sites in proteins.

The secondary structure of wild-type and mutant αB-crystallins was determined by far-UV CD spectral analysis. The far-UV CD spectra (Figure 8) for wild-type αB and αBR50G were similar, indicating no change in their secondary structure. On the other hand, the far-UV profile of αBP51A showed increased α-helical content as opposed to the wild type and αBR50G. This finding implies that mutation of P51A significantly altered the structure of αB, whereas charge replacement (R50G) did not have any effect on the secondary structure of the protein. Near-UV CD profiles for wild type and αB mutants were not significantly different (data not shown). This indicates that neither charge replacement nor increased α-helicity due to P51A mutation caused any tertiary structural changes.

The stability of wild-type αB and its mutants was determined by measuring light scattering of the proteins at both 37 and 43 °C, the temperatures used in the chaperone assays. At both of these temperatures, neither the wild type nor the mutants showed any light scattering or aggregation, indicating that the mutation did not alter protein stability (data not shown).

Functional Characterization of αB Mutants. The ability of mutant proteins to suppress either thermal or EDTA-induced aggregation of target proteins was analyzed. Figure 9A shows the thermal aggregation of CS (75 μg) at 43 °C in the presence of both wild-type and mutant proteins at different concentrations. The wild type (50 μg) and αBR50G (35 μg) completely suppressed the aggregation of CS, but αBP51A at both 35 and 50 μg showed reduced chaperone-like activity. EDTA facilitates aggregation of ADH at 37 °C, which otherwise needs higher temperature for aggregation. EDTA-induced aggregation of ADH (0.8 mg) in the presence of 20 μg each of wild-type αB, αBP51A, and αBR50G (Figure 9B) shows that αBP51A could not com-

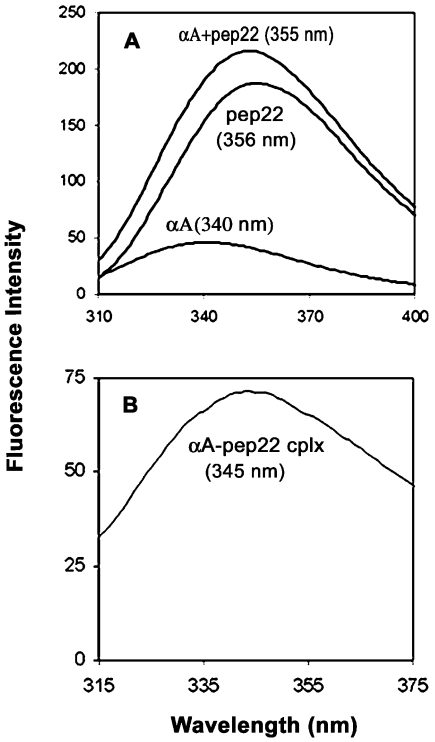

FIGURE 4: Intrinsic fluorescence spectra of a mixture of αA-crystallin and αB-crystallin peptide (peptide 22). (A) At 0 time and (B) the αA-crystallin−peptide 22 complex isolated from the gel filtration column following a 16 h incubation at 37 °C. The spectra were recorded using a Jasco FP 750 spectrofluorometer (Ex 295 nm; bandwidth of 5 nm for Ex and Em modes). Wavelength emission maxima for each sample are indicated in parentheses.

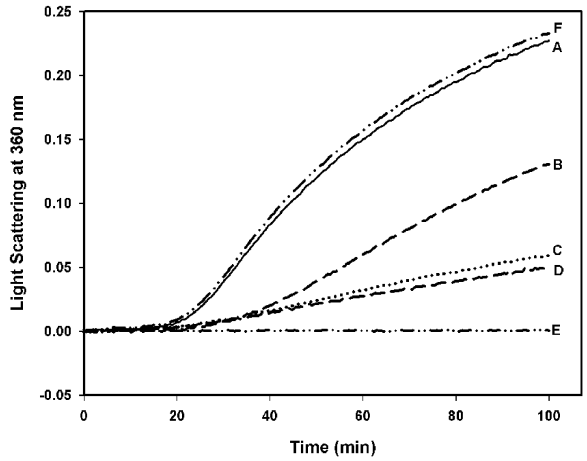

FIGURE 5: Chaperone-like activity of the αA−RS-1 peptide complex against EDTA-induced aggregation of ADH. Experimental details are included in the text. Key: (A) ADH (400 μg), (B) ADH + 20 μg of the αA−RS-1 peptide complex, (C) ADH + 45 μg of αA, (D) ADH + 45 μg of the αA−RS-1 peptide complex, (E) 50 μg of RS-1 peptide alone, and (F) ADH + 50 μg of RS-1 peptide.

pletely suppress the aggregation of ADH, while αBR50G showed chaperone-like function similar to wild type.

The effect of mutation on subunit exchange was examined by FRET assay. Wild-type αB, αBP51A, and αBR50G were labeled with Alexa fluor 350, and they act as energy donors, and αA was labeled with Alexa fluor 488, and it acts as an energy acceptor. The fluorescent αA-488 and αB-350 (wild type/mutant) mixture was prepared in 3:1 ratio to mimic the in vivo situation (*11*). We allowed the subunit exchange to

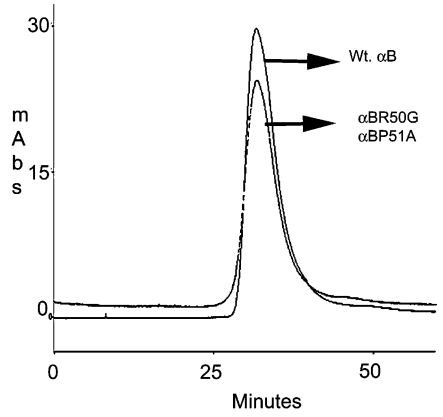

FIGURE 6: Gel filtration profiles of wild-type and mutant αB-crystallins on a SEC 4000 column.

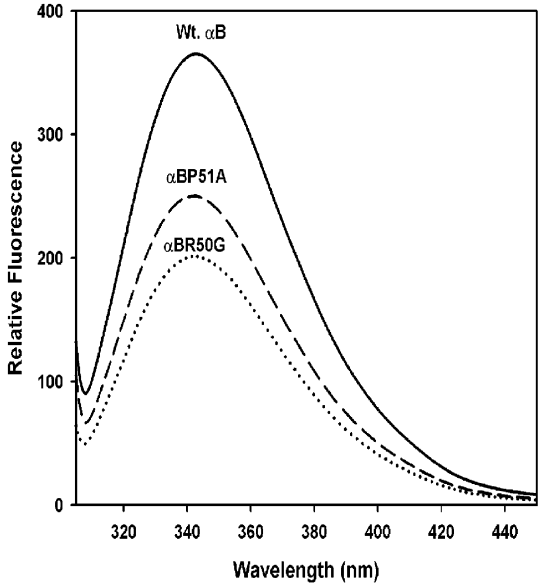

FIGURE 7: Intrinsic tryptophan fluorescence spectra for wild-type and αB-crystallin mutants. Protein samples (200 μg) in phosphate buffer were excited at 295 nm.

proceed at 37 °C in PBS for 2 h. The time-dependent decrease in donor fluorescence and concomitant increase in the acceptor fluorescence were monitored upon exciting the samples at the donor absorption maximum (346 nm). After curve fitting of the raw data and nonlinear regression analysis (using Sigmaplot 8.0 software), we then calculated the subunit exchange rate (Figure 10A). For αB−αA interaction, the rate of subunit exchange was calculated as 13.84×10^{-4} s^{-1}, for αBR50G−αA interaction, it was 10.89×10^{-4} s^{-1}, and for αBP51A−αA interaction, the exchange rate was 5.2×10^{-4} s^{-1}. The P51A mutation reduced the rate of subunit exchange by 63%, whereas R50G reduced the subunit exchange rate by 23%.

We examined the ability of αBP51A and αBR50G to replace wild-type αB from the αB−αA oligomer. For this purpose, a heterooligomer was allowed to form between αA-488 and αB (unlabeled) for 4 h at 37 °C. The FRET assay was then started by the addition of αBR50G labeled with Alexa 350 (25 μg) or αBP51A labeled with Alexa 350 (25 μg), and the subunit exchange was monitored for 3 h. αB labeled with Alexa 350 (25 μg) was used as a control. Because of the dynamic nature of α-crystallin subunits, αB-350 readily replaced unlabeled αB (Figure 10B). When

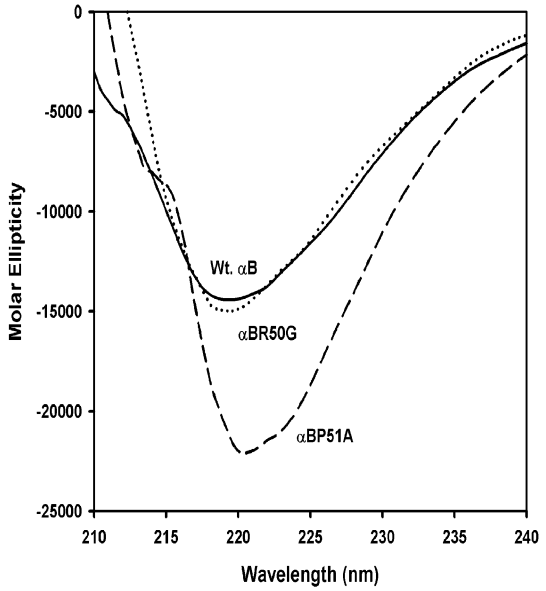

FIGURE 8: Far-UV CD spectra of wild-type and mutant αB-crystallins. Spectra were recorded at a protein concentration of 200 μg/mL using a 0.05 cm path length cell.

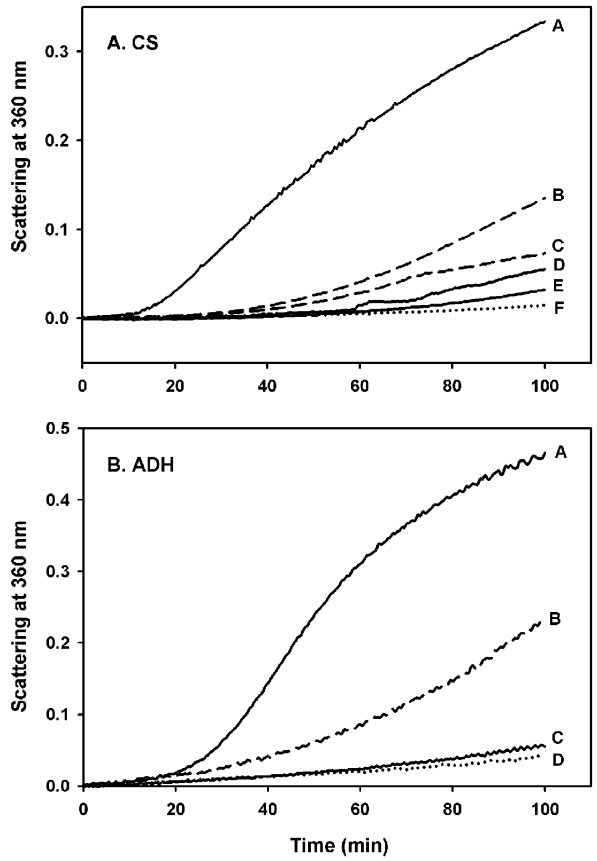

FIGURE 9: Chaperone-like activity of wild-type αB and mutants of αB-crystallin against aggregation of CS (A) and ADH (B). Experimental details are included in the text. Upper panel (A): (A) CS (75 μg), (B) CS + 35 μg of αBP51A, (C) CS + 50 μg of αBP51A, (D) CS + 35 μg of wild-type αB, (E) CS + 50 μg of wild-type αB, and (F) CS + 35 μg of αBR50G. Lower panel (B): (A) ADH (800 μg), (B) ADH + 20 μg of αBP51A, (C) ADH + 20 μg of wild-type αB, and (D) ADH + 20 μg of αBR50G.

compared to αB-350, αBR50G-350 replaced αB at a 12.5% reduced rate. On the other hand, αBP51A replaced αB at a very low rate (55% reduction), corroborating the previous observation about its slow subunit exchange with αA (Figure 10A).

We also investigated whether RS-1 peptide could compete with αBR50G or αBP51A for interaction with αA. The subunit exchange study was performed by incubation of αBP51A-350 or αBR50G-350 (25 μg), αA-488 (75 μg), and unlabeled αB (25 μg) at 37 °C for 3 h. As α-crystallin subunits exchange continuously, unlabeled αB effectively competes with αBR50G-350 or αBP51A-350 for interaction with αA. Thus, less energy is transferred to αA (this served as a control). RS-1 peptide (unlabeled) was used at concentrations of 75 and 100 μg (Figure 10C,D). Similar to αB, RS-1 peptide also effectively competed with αBR50G (Figure 10C) and αBP51A (Figure 10D), indicating that RS-1 is one of the interacting sites between αB- and αA-crystallins.

DISCUSSION

By using a combination of mutagenesis and spin-labeling studies, it was suggested earlier that the α-crystallin domain may be involved in subunit interaction (*33*). On the basis of deletion studies, it appears that the N-terminal region in αA- and αB-crystallin may play a role in aggregate formation (*17*). The phosphorylation−oligomerization study with HSP 27 also revealed that the N-terminal domain is essential for oligomerization while the C-terminal domain plays a role in dimerization (*34*). αB-crystallin has three phosphorylation sites: Ser 19, 45, and 59 (*35*). The Ser 45 and 59 reside at recognition sites 1 and 2 identified in this study (Figure 1). Therefore, we hypothesize that phosphorylation-induced disaggregation of αB-crystallin [reported earlier by Ito et al. (*36*)] may arise due to the interference of the phosphate moiety on Ser 45 or 59, which otherwise is involved in interaction with another subunit.

In our study, 20-mer αB-crystallin peptides were immobilized on PVDF membrane. These were longer than the peptides used in many earlier studies (*25*−*27*). We used 20-mer peptide arrays for the following reason. Earlier, we discovered that a 19-mer αA peptide interacts with a number of denaturing proteins and therefore has the adequate structure to interact with other proteins (*37*). Therefore, we hypothesized that an array made of 19-residue peptides would be sufficient to determine an interaction between αA- and αB-crystallin. The immobilized αB-crystallin peptides that interacted with αA-crystallin were the peptides at spots 20−22, 27−31, 45, and 53, spanning residues 38−79 and 88−123 (Figure 1). Because only 10 of the 79 peptides in the scan reacted with αA, the interaction appears to be specific. On the basis of above data, residues 42−57 and 60−71 in αB-crystallin can be called αA-crystallin recognition sites. Recently, using a pin array system Clark et al. (*38*) also reported that the 41−57 region in αB-crystallin is involved in interaction with crystallins and substrate proteins.

The RS-2 sequence (residues 60−71) overlaps with a region (from residues 57−69) identified earlier in our laboratory as the sequence in αB-crystallin that interacted with SAED-labeled ADH during chaperone-like action (*39*). However, results from mellitin and bis-ANS binding studies (*37*, *40*) led us to propose that residues 73−82 in αB-crystallin contribute to a chaperone site. This was later confirmed by the chaperone-like activity displayed by the

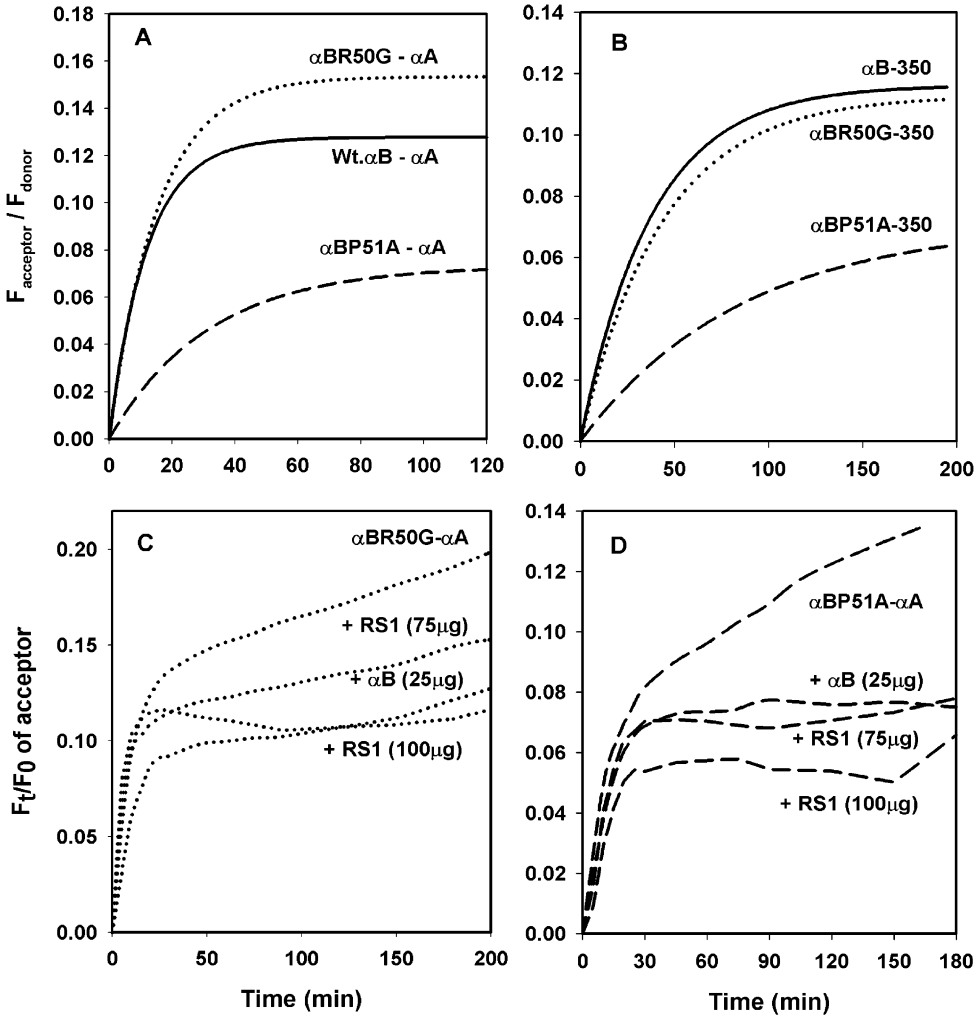

FIGURE 10: Subunit exchange studies of wild-type αB and αB-crystallin mutants with αA-crystallin. **(**A) 25 μg of αB-crystallin-350 (wild-type/mutants) was used as the energy donor, and 75 μg of αA-488 was the energy acceptor. $F_{acceptor}/F_{donor}$ represents the ratio of fluorescence intensities at 520 to 436 nm. (B**)** An oligomer was preformed between αB-crystallin (25 μg, unlabeled) and αA-crystallin-488 (75 μg) at 37 °C for 4 h. 25 μg each of αB-350, αBP51A-350, and αBR50G-350 was added to initiate competition between unlabeled αB and labeled wild-type and mutant αB-crystallins for interaction with αA-488. (C**)** Effect of RS-1 peptide on subunit exchange between αBR50G-350 and αA-488 and (D**)** between αBP51A-350 and αA-488. 25 μg each of αBR50G-350 and αBP51A-350 was mixed with 75 μg of αA-488 in PBS. 25 μg of wild-type (unlabeled) αB-crystallin as a control or RS1 peptide at 75 and 100 μg was added. The competition between RS1 peptide and αBR50G-350 or αBP51A-350 for interaction with αA-488 was monitored by measuring the ratio of fluorescence intensity at 520 nm of the acceptor (αA-488) at given time intervals to the fluorescence at the beginning of the assay (F_t/F_0).

synthetic peptide DRFSVNLDVKHFSPEELKVK comprising the 73−92 region of αB-crystallin (*41*). But a synthetic peptide comprising residues 57−69 of αB-crystallin failed to show any chaperone-like function (unpublished results). Therefore, the SAED-labeled ADH interacting region in αB-crystallin appears to be a chaperone site flanking region rather than the actual chaperone site by itself. Additionally, during the initial study (*39*), the terminal photoactive azidocoumarin moiety on a 23.6 Å spacer arm may have reacted with residues proximal to the actual chaperone site, the 73−92 region of αB-crystallin. Taken together, it appears that the 60−71 region of αB-crystallin, while serving as a subunit interaction site, also functions as a chaperone site flanking region.

The entire C-terminal domain of αB-crystallin has been shown to be involved in interaction with αA-crystallin using two hybrid systems (*19*, *20*). But our peptide scan study did not pick up any peptides in the C-terminal region of αB-crystallin. While the reason for this discrepancy is not known, we hypothesize that the presence of discontinuous or conformation-dependent binding sites, where the key residues are distributed over two or more binding regions that are separated in the primary structure, may be contributing to subunit interactions in the C-terminal domain. In native protein, amino acids at different locations may be brought together on the protein surface to form a composite epitope (binding site). But peptides covering only one portion of the binding region, as synthesized in a scan of overlapping peptides, may have very low affinities for the interacting proteins. This may be responsible for our inability to detect αA interaction sites in the C-terminal region of αB-crystallin.

A combination of gel filtration and HPLC chromatography studies (Figure 3) confirmed the interaction of αB-crystallin peptide (RS-1) with αA-crystallin. We estimated that the peptide and αA-crystallin bind in 1:2 ratio (peptide:αA-crystallin subunit). While there is a potential for each subunit of αA-crystallin to bind one peptide, the oligomeric nature of αA subunits may be restricting the binding of one RS-1 peptide per subunit. Since the reverse sequence of RS-1 peptide and a hydrophobic N-terminal peptide (1−18) of αB-

crystallin failed to bind to αA-crystallin, the binding of RS-1 peptide to αA-crystallin appears to be sequence-specific rather than a function of hydrophobicity. The Trp residues in peptides generally show fluorescence emission spectra, with a peak around the 355−360 nm region, similar to the Trp residues in aqueous media or in fully denatured proteins. However, interaction of peptides possessing Trp residues with proteins would result in diminished exposure of the peptide Trp to the aqueous environment with a concomitant blue shift in the fluorescence emission maxima. The fluorescence spectra for the peptide 22−αA-crystallin complex isolated by gel filtration showed an emission maximum at 345 nm (Figure 4B). This emission at 345 nm is at a higher wavelength than for αA-crystallin by itself and at a significantly lower wavelength than for the peptide Trp. This suggests the association of the αB peptide containing a partially exposed Trp residue with αA-crystallin. Taken together, these data confirm the interaction of the TSLSP-FYLRPPSFLRAPSWF sequence in αB-crystallin with αA-crystallin.

Previous studies have shown that residues at the beginning of the αA-crystallin domain are involved in the interaction with target proteins during chaperone action (*37*). A site-directed mutagenesis study confirmed this interaction (*32*). Other studies have shown that mutation of other residues results in loss/gain of chaperone-like activity (*42*−*47*). Since both homoaggregates and heteroaggregates of αA-crystallin and αB-crystallin show chaperone-like activity (*4*) and can form complexes with denaturing proteins, it appears that the subunit interaction region and the chaperone site are apparently distinct. The two regions, however, can reside in the same domain. Our studies on the chaperone-like function of the αA-crystallin−RS-1 complex reveal the same. Binding of RS-1 peptide does not alter the chaperone-like activity of αA-crystallin (Figure 5), thus confirming that the subunit interaction region and the chaperone site are very distinct.

Earlier studies have shown that the N-terminal region and the α-crystallin domain are involved in subunit interactions (*17*, *33*). Deletion of the first 19 residues does not alter the size of αA-crystallin and the rate of subunit exchange (*8*). In contrast, deletion of first 56 residues results in a drastic reduction in the size leading to the formation of dimers or tetramers and the failure of protein to exchange subunits (*8*). On the other hand, deletion of nine residues in αA- (20−28 residues) and αB-crystallins (21−29 residues), the conserved SRLFDQFFG sequence, alters the oligomer formation but does not lead to the formation of dimers and trimers (*43*). These deletion mutants also exhibit an increased subunit exchange rate, compared to their wild-type counterparts (*43*). Therefore, it appears that interacting regions for oligomer formation lie in the first 19−56 amino acids. Our peptide scan data show that residues 42−57 (RS-1) contribute to one of the interacting sites between αB- and αA-crystallins. Therefore, it was imperative to investigate the residues in the RS-1 region that will be essential for subunit interactions.

The R50G and P51A mutations did not show any effect on the homooligomerization of the proteins (Figure 6). The wild-type αB-crystallin and the purified mutant proteins show a molecular size of ∼610 kDa. The Trp emission maximum of both wild-type and mutant proteins was similar (343 nm, Figure 7). However, there was a reduction in the intensity of Trp emission for mutants as compared to wild type, indicating that the mutation has altered the microenvironment of the Trp residues. This change most probably affected Trp^{60} as it is very close to the RS-1 region (42−57 residues).

The effect of mutation in the RS-1 region on the secondary structure of the proteins was investigated by far-UV CD spectra (Figure 8). αB-Crystallin mainly exhibits β-sheet structure with a minor content of α-helix (*47*). Figure 8 shows that the P51A mutation increased the α-helical structure of the protein, whereas charge replacement (R50G) had no effect on the secondary structure. Additionally, the αBP51A mutant also showed increased negative ellipticity, which is known to be associated with helical structure. On the other hand, near-UV CD profiles for wild-type αB, αBP51A, and αBR50G were similar (data not shown), suggesting that the mutation had an insignificant effect on the tertiary structure of the proteins. The change observed in tryptophan emission spectra is not reflected in the near-UV CD profiles as absorption by Trp residues is masked by that of Tyr residues.

To investigate whether the change in structure translated into a change in function of the mutants, we analyzed their chaperone-like function as well as their subunit interaction with αA-crystallin. Compared to wild-type αB and αBR50G (Figure 9), the αBP51A mutant showed reduced chaperone-like activity. Since all of the proteins exhibited similar hydrophobicity, decreased chaperone-like function of αBP51A could be a result of its altered structure.

The hallmark of all sHSPs is their tendency to assemble into oligomers of high molecular masses. Oligomerization is a structural prerequisite for the chaperone function in a majority of sHSPs (*8*, *10*). We investigated whether mutation in the RS-1 region affects the dynamic nature of αB-crystallin and its mutants (i.e., their subunit exchange with αA-crystallin). The subunit exchange was monitored using FRET assay, and the rate of subunit exchange was calculated from the initial slopes for each curve. Figure 10A shows that, for the αBP51A−αA interaction, the exchange rate was reduced by 63% when compared to the wild-type αB−αA interaction. The αBR50G−αA interaction proceeded with 23% reduction in the subunit exchange rate when compared to the αB−αA interaction. Our results indicate that structural alteration caused by mutation of P51A in αB significantly affected the subunit exchange rate whereas charge replacement did not result in a similar change.

We also investigated the ability of mutant proteins to replace wild-type αB from a preformed heterooligomer with αA-αB crystallins. Figure 10B shows that αBR50G replaces wild-type αB at a slightly reduced rate (12.5% reduction as compared to wild-type αB); αBP51A replaces wild-type αB at 55% slower rate than the wild type. This observation corroborates the result shown in Figure 10A, suggesting that P51A mutation alters the structure of αB in such a way that heterooligomer formation is hindered. However, complete cessation of subunit exchange was not observed as the P51A mutation was created in only one of the recognition sites identified from the peptide scan. We hypothesize that complete disruption of subunit interaction may require simultaneous mutation at all recognition sites. This reveals that multiple sites are involved in subunit interactions. This was also suggested earlier by Bova et al. (*7*) on the basis of the high activation energy (relative to other exchange reactions) obtained for the αA−αA interaction. Nevertheless,

our study implies that the RS-1 region plays a major role in subunit interaction between αA- and αB-crystallins.

If the RS-1 region is one of the interacting regions between αA- and αB-crystallins during subunit exchange, RS-1 peptide should competitively inhibit the interaction between αB- and αA-crystallins. On the basis of our experimental results with different RS-1 concentrations on subunit exchange between αBP51A-αA and αBR50G-αA (Figure 10C,D), we deduce that RS-1 peptide effectively competes with αBP51A and αBR50G for interaction with αA.

On the basis of the above study, we conclude that the RS-1 region comprising residues 42−57 in the N-terminal region of αB-crystallin is involved in the interaction with αA-crystallin. Upon binding to the RS-1 peptide, αA-crystallin does not lose its chaperone-like activity, thus confirming that the subunit interaction site and chaperone site are different. Mutation involving charge replacement does not cause any considerable structural and functional changes. On the other hand, replacement of Pro with Ala significantly alters the structure and function of the protein. Therefore, the RS-1 region is one of the critical motifs that contribute to the oligomerization or subunit interactions in αB-crystallin.

ACKNOWLEDGMENT

We are grateful to Dr. Lixing Reneker for help in the course of this study.

REFERENCES

1. de Jong, W. W., Caspers, G. J., and Leunissen, J. A. (1998) Genealogy of the alpha-crystallin−small heat-shock protein superfamily, *Int. J. Biol. Macromol. 22*, 151−162.
2. Horwitz, J. (1992) Alpha-crystallin can function as a molecular chaperone, *Proc. Natl. Acad. Sci. U.S.A. 89*, 10449−10453.
3. Merck, K. B., Groenen, P. J., Voorter, C. E., de Haard-Hoekman, W. A., Horwitz, J., Bloemendal, H., and de Jong, W. W. (1993) Structural and functional similarities of bovine alpha-crystallin and mouse small heat-shock protein. A family of chaperones, *J. Biol. Chem. 268*, 1046−1052.
4. Horwitz, J. (2003) Alpha-crystallin, *Exp. Eye Res. 76*, 145−153.
5. Groenen, P. J., Merck, K. B., de Jong, W. W., and Bloemendal, H. (1994) Structure and modifications of the junior chaperone alpha-crystallin. From lens transparency to molecular pathology, *Eur. J. Biochem. 225*, 1−19.
6. Sun, T. X., Akhtar, N. J., and Liang, J. J. (1998) Subunit exchange of lens alpha-crystallin: a fluorescence energy transfer study with the fluorescent labeled alphaA-crystallin mutant W9F as a probe, *FEBS Lett. 430*, 401−404.
7. Bova, M. P., Ding, L. L., Horwitz, J., and Fung, B. K. (1997) Subunit exchange of alphaA-crystallin, *J. Biol. Chem. 272*, 29511−29517.
8. Bova, M. P., McHaourab, H. S., Han, Y., and Fung, B. K. (2000) Subunit exchange of small heat shock proteins. Analysis of oligomer formation of alphaA-crystallin and Hsp27 by fluorescence resonance energy transfer and site-directed truncations, *J. Biol Chem. 275*, 1035−1042.
9. van den Oetelaar, P. J., van Someren, P. F., Thomson, J. A., Siezen, R. J., and Hoenders, H. J. (1990) A dynamic quaternary structure of bovine alpha-crystallin as indicated from intermolecular exchange of subunits, *Biochemistry 29*, 3488−3493.
10. Narberhaus, F. (2002) Alpha-crystallin-type heat shock proteins: socializing minichaperones in the context of a multichaperone network, *Microbiol. Mol. Biol. Rev. 66*, 64−93.
11. Sun, T. X., and Liang, J. J. (1998) Intermolecular exchange and stabilization of recombinant human alphaA- and alphaB-crystallin, *J. Biol. Chem. 273*, 286−290.
12. Han, Y., and Fung, B. K. K. (2000) Orientation of αA-crystallin oligomer as determined by fluorescence spectroscopy, *Invest. Ophthalmol. Visual Sci. 41*, S748.
13. Brady, J. P., Garland, D., Duglas-Tabor, Y., Robison, W. G., Jr., Groome, A., and Wawrousek, E. F. (1997) Targeted disruption of the mouse alpha A-crystallin gene induces cataract and cytoplasmic inclusion bodies containing the small heat shock protein alpha B-crystallin, *Proc. Natl. Acad. Sci. U.S.A. 94*, 884−889.
14. Srinivas, V., Santhoshkumar, P., and Sharma, K. K. (2002) Effect of trifluoroethanol on the structural and functional properties of alpha-crystallin, *J. Protein Chem. 21*, 87−95.
15. Kim, K. K., Kim, R., and Kim, S. H. (1998) Crystal structure of a small heat-shock protein, *Nature 394*, 595−599.
16. van Montfort, R. L., Basha, E., Friedrich, K. L., Slingsby, C., and Vierling, E. (2001) Crystal structure and assembly of a eukaryotic small heat shock protein, *Nat. Struct. Biol. 8*, 1025−1030.
17. Merck, K. B., De Haard-Hoekman, W. A., Oude Essink, B. B., Bloemendal, H., and De Jong, W. W. (1992) Expression and aggregation of recombinant alpha A-crystallin and its two domains, *Biochim. Biophys. Acta 1130*, 267−276.
18. Kokke, B. P., Leroux, M. R., Candido, E. P., Boelens, W. C., and de Jong, W. W. (1998) *Caenorhabditis elegans* small heat-shock proteins Hsp12.2 and Hsp12.3 form tetramers and have no chaperone-like activity, *FEBS Lett. 433*, 228−232.
19. Liu, C., and Welsh, M. J. (1999) Identification of a site of Hsp27 binding with Hsp27 and alpha B-crystallin as indicated by the yeast two-hybrid system, *Biochem. Biophys. Res. Commun. 255*, 256−261.
20. Fu, L., and Liang, J. J. (2002) Detection of protein−protein interactions among lens crystallins in a mammalian two-hybrid system assay, *J. Biol. Chem. 277*, 4255−4260.
21. Fu, L., and Liang, J. J. (2003) Alteration of protein−protein interactions of congenital cataract crystallin mutants, *Invest. Ophthalmol. Visual Sci. 44*, 1155−1159.
22. MacRae, T. H. (2000) Structure and function of small heat shock/alpha-crystallin proteins: established concepts and emerging ideas, *Cell. Mol. Life Sci. 57*, 899−913.
23. Frank, R. (2002) The SPOT-synthesis technique. Synthetic peptide arrays on membrane supports−principles and applications, *J. Immunol. Methods 267*, 13−26.
24. Rudiger, S., Germeroth, L., Schneider-Mergener, J., and Bukau, B. (1997) Substrate specificity of the DnaK chaperone determined by screening cellulose-bound peptide libraries, *EMBO J. 16*, 1501−1507.
25. Yoshioka, N., and Atassi, M. Z. (1999) Subunit interacting surfaces of human hemoglobin in solution: localization of the alpha-beta subunit interacting surfaces on the alpha-chain by a comprehensive synthetic strategy, *J. Protein Chem. 18*, 179−185.
26. Reineke, U., Sabat, R., Misselwitz, R., Welfle, H., Volk, H. D., and Schneider-Mergener, J. (1999) A synthetic mimic of a discontinuous binding site on interleukin-10, *Nat. Biotechnol. 17*, 271−275.
27. Reineke, U., Sabat, R., Volk, H. D., and Schneider-Mergener, J. (1998) Mapping of the interleukin-10/interleukin-10 receptor combining site, *Protein Sci. 7*, 951−960.
28. Chou, P. Y. (1989) Prediction of protein structural classes from amino acid compositions, in *Prediction of Protein Structures and the Principles of Protein Conformation* (Fasman, G. D., Ed.) pp 549−586, Plenum Publishing Corp., New York.
29. Bhattacharyya, J., Srinivas, V., and Sharma, K. K. (2002) Evaluation of hydrophobicity versus chaperonelike activity of bovine alphaA- and alphaB-crystallin, *J. Protein Chem. 21*, 65−71.
30. Towbin, H., Staehelin, T., and Gordon, J. (1979) Electrophoretic transfer of proteins from polyacrylamide gels to nitrocellulose sheets: procedure and some applications, *Proc. Natl. Acad. Sci. U.S.A. 76*, 4350−4354.
31. Horwitz, J., Huang, Q. L., Ding, L., and Bova, M. P. (1998) Lens alpha-crystallin: chaperone-like properties, *Methods Enzymol. 290*, 365−383.
32. Santhoshkumar, P., and Sharma, K. K. (2001) Phe71 is essential for chaperone-like function in alpha A-crystallin, *J. Biol. Chem. 276*, 47094−47099.
33. Berengian, A. R., Parfenova, M., and McHaourab, H. S. (1999) Site-directed spin labeling study of subunit interactions in the alpha-crystallin domain of small heat-shock proteins. Comparison of the oligomer symmetry in alphaA-crystallin, HSP 27, and HSP 16.3, *J. Biol. Chem. 274*, 6305−6314.
34. Lambert, H., Charette, S. J., Bernier, A. F., Guimond, A., and Landry, J. (1999) HSP27 multimerization mediated by phosphorylation-sensitive intermolecular interactions at the amino terminus, *J. Biol. Chem. 274*, 9378−9385.

35. Ito, H., Okamoto, K., Nakayama, H., Isobe, T., and Kato, K. (1997) Phosphorylation of alphaB-crystallin in response to various types of stress, *J. Biol. Chem. 272*, 29934−29941.
36. Ito, H., Kamei, K., Iwamoto, I., Inaguma, Y., Nohara, D., and Kato, K. (2001) Phosphorylation-induced change of the oligomerization state of alpha B-crystallin, *J. Biol. Chem. 276*, 5346−5352.
37. Sharma, K. K., Kumar, R. S., Kumar, G. S., and Quinn, P. T. (2000) Synthesis and characterization of a peptide identified as a functional element in alphaA-crystallin, *J. Biol. Chem. 275*, 3767−3771.
38. Clark, J. I., Estrada, M. R., and Ghosh, J. G. (2004) Interaction sites in human alphaB crystallin mediate multiple functions, *Invest. Ophthalmol. Visual Sci. 45* (E-Abstract 3976).
39. Sharma, K. K., Kaur, H., and Kester, K. (1997) Functional elements in molecular chaperone alpha-crystallin: identification of binding sites in alpha B-crystallin, *Biochem. Biophys. Res. Commun. 239*, 217−222.
40. Sharma, K. K., Kumar, G. S., Murphy, A. S., and Kester, K. (1998) Identification of 1,1′-bi(4-anilino)naphthalene-5,5′-disulfonic acid binding sequences in alpha-crystallin, *J. Biol. Chem. 273*, 15474−15478.
41. Sharma, K. K., Puttur, S., and Bhattacharrya, J. (2002) Characterization of alpha B crystallin chaperone site, *Exp. Eye Res. 72* (Suppl. 2), 34.
42. Bova, M. P., Yaron, O., Huang, Q., Ding, L., Haley, D. A., Stewart, P. L., and Horwitz, J. (1999) Mutation R120G in alphaB-crystallin, which is linked to a desmin-related myopathy, results in an irregular structure and defective chaperone-like function, *Proc. Natl. Acad. Sci. U.S.A. 96*, 6137−6142.
43. Pasta, S. Y., Raman, B., Ramakrishna, T., and Rao, Ch. M. (2003) Role of the conserved SRLFDQFFG region of alpha-crystallin, a small heat shock protein. Effect on oligomeric size, subunit exchange, and chaperone-like activity, *J. Biol. Chem. 278*, 51159−51166.
44. Smulders, R. H., Merck, K. B., Aendekerk, J., Horwitz, J., Takemoto, L., Slingsby, C., Bloemendal, H., and De Jong, W. W. (1995) The mutation Asp69→Ser affects the chaperone-like activity of alpha A-crystallin, *Eur. J. Biochem. 232*, 834−838.
45. Plater, M. L., Goode, D., and Crabbe, M. J. (1996) Effects of site-directed mutations on the chaperone-like activity of alphaB-crystallin, *J. Biol. Chem. 271*, 28558−28566.
46. Bera, S., and Abraham, E. C. (2002) The alphaA-crystallin R116C mutant has a higher affinity for forming heteroaggregates with alphaB-crystallin, *Biochemistry 41*, 297−305.
47. Kelley, P. B., and Abraham, E. C. (2003) Thermally induced disintegration of the oligomeric structure of alphaB-crystallin mutant F28S is associated with diminished chaperone activity, *Mol. Cell. Biochem. 252*, 273−278.

BI048151S